Table 1. Herbicidal activity of 1 (R=2-Cl-allyl) on grasses 20 days after post-emergence treatment

	Control (%)											
$g\,ha^{-1}$	Maize	Wheat	Barley	Cotton	Signal grass	Bamyard grass	Johnson grass	Green foxtail	Black grass	Wild oat	Annual meadow grass	Yellow nut-sedge
800	92	95	89	89	95	95	89	95	95	95	95	78
200	89	92	89	83	95	94	92	94	86	92	92	42
50	72	83	86	36	83	92	69	92	86	81	92	11

In-vitro inhibition constants were determined for the majority of analogs in a standard assay with partially purified AHAS enzyme from etiolated maize shoots. The best inhibitors achieved IC_{50} values of 0.16 –0.35 μM. This is well within the range of those of commercial herbicides (chlorsulfuron IC_{50} = 8.5 nM; flumetsulam IC_{50} = 0.1 μM; imazethapyr IC_{50} = 3.5 μM). The in-vitro data correlated well with the activity ranking observed in the greenhouse. The kinetics of the enzyme inhibition were studied in more detail for one analog (**1**, R_1 = isobutyl). As with other classes of AHAS inhibitor, a slow tight binding characteristic was found and higher inhibition was measured after 30–40 min incubation.

In a simple qualitative model of binding to AHAS, the pyrimidine rings of different known inhibitors were superimposed. The conformation of the remainder of the molecule (in the anionic form) was then optimized for binding to a putative positive centre which was fixed in space. The results for the pyrazolinones suggest that the pyrimidine ring at N-1 is equivalent to that of other inhibitors. The second pyrimidine at C-4 participates in binding to the positive centre, with the negative charge of the anion being delocalized into the ring.

3. CONCLUSIONS

Although the pyrazolinones did not achieve commercially useful herbicidal activity *in vivo*, they constitute a novel class of intrinsically potent AHAS inhibitors with some unique structural features. SAR suggests the presence of a second binding niche on the enzyme for a 4,6-dimethoxypyrimidine ring, in close proximity to the binding site of the acidic functionality of the inhibitors.

Temperature-insensitive microemulsions and dilution ripening

PD Fletcher,[1] BP Binks,[1] DJF Taylor,[1] P Taylor,[2]*
DK Rodham[2] and PD Winn[2]
[1]*Surfactant Science Group, University of Hull, Hull, HU6 7RX, UK*
[2]*Zeneca Agrochemicals, Jealott's Hill Research Station, Bracknell, Berkshire, RG42 6ET, UK*

* Correspondence to: P Taylor, Zeneca Agrochemicals, Jealott's Hill Research Station, Bracknell, Berks RG42 6ET, UK
(*Received 1 July 1998; accepted 1 February 1999*)

Abstract: Single-phase microemulsions are thermodynamically stable dispersions of an oil in water (O/W) or water in oil (W/O) and are an attractive means of formulating agrochemical products (bicontinuous systems of mutually dispersed oil and water are also possible). Two areas of interest are reported in this summary. (i) Temperature sensitivity – a disadvantage of many microemulsion systems is that the phase boundary of the single-phase region is often highly dependent upon temperature and electrolyte concentration. The aim of this work was the production of temperature-insensitive systems, the criterion used being that the radius of curvature of the droplets at the solubilisation boundary was independent of temperature. (ii) The application of microemulsion systems will involve dilution into water to form the spray system and, as such, an understanding of how the droplets grow under these conditions is of importance. Factors affecting droplet growth processes occurring upon dilution into water have been investigated.

Keywords: microemulsions; temperature sensitivity; dilution ripening

The phase behaviour of microemulsions (and hence solubilisation capacity) is dominated by the curvature of the surfactant layer around the droplets. At the solubilisation phase boundary the curvature of the interface is the 'natural' curvature for that set of experimental conditions, and close to the Phase Inversion Temperature (PIT) this curvature scales linearly with temperature for many surfactants. The natural curvature is determined by the relative sizes of the headgroup and the tail of the surfactant. If these are similar in size, large droplets are formed, whilst increasing the relative size of the headgroup or the tail will result in smaller O/W or W/O droplets respectively.

Plots of the reciprocal of the natural radius (curvature) versus temperature have been determined for heptane/ 60 mM sodium chloride microemulsions stabilised by Aerosol OT (AOT) and dodecyl pentaoxyethylene glycol ether ($C_{12}E_5$) and their mixtures. The radii of curvature were estimated from the extent of solubilisation. All of the plots were linear, with the reciprocal of r_{nat} decreasing with temperature for the non-ionic surfactant and increasing for the ionic surfactant; mixtures showed intermediate slopes. The oppositely signed slopes arise from the fact that increasing temperature shrinks the headgroups of

nonionic surfactants (by dehydration of the hydrophilic group) while it swells ionic headgroups, possibly through increased dissociation of the ions.

The opposite behaviour shown by the two types of surfactant suggests a means to form temperature-insensitive systems, in that, at a particular AOT: $C_{12}E_5$ ratio, the natural radius should be independent of temperature. The linear plots obtained above show that:

$$1/r_{\text{nat}} = sT + i \quad (1)$$

where s is the slope and i the intercept of the line, both dependent on X (the weight fraction of AOT in the mixture) and can be accurately represented by

$$s = s_{\text{AOT}}X + s_{C_{12}E_5}(1-X) + B_sX(1-X) \quad (2)$$

$$i = i_{\text{AOT}}X + i_{C_{12}E_5}(1-X) + B_iX(1-X) \quad (3)$$

B_s and B_i are fitting parameters (s refers to the slope and i to the intercept) and these have been obtained for a range of compositions and have been used to give a surface plot of r_{nat} as a function of both temperature and composition. The surface obtained in this way shows a number of features. Areas in which the natural radius changes rapidly from positive to negative represent the phase inversion from O/W (positive radius) to W/O (negative). More importantly, it is possible to identify temperature-insensitive regions from the plot as the flat areas lying between the phase-inversion regions. For the particular system studied, the radius is essentially independent of T at $X = 0.62$; this has been observed experimentally and predicted analytically from the above equations. Thus, by using the above equations to model the behaviour of this system we can predict the necessary composition required for temperature insensitivity. The model is also able to explain PITs, interfacial tensions and maximum solubilisation in these systems.[1] The extent of solubilisation for a temperature-independent system can be independently optimised by addition of salt.[1]

Dilution of an O/W microemulsion into water results in it becoming thermodynamically unstable and the droplets will tend to grow to reduce their interfacial energy.[2] The process responsible for this growth at high dilutions is most likely to be Ostwald ripening. In this context, we have referred to the process as dilution ripening. Ostwald ripening arises from the fact that small droplets are more soluble than larger ones due to the Kelvin effect, so that small droplets tend to dissolve and the dissolved material diffuses through the aqueous phase and redeposits on larger droplets. The rate of ripening is dependent upon the solubility and diffusion coefficient of the oil in water, the interfacial tension between the oil and water and also on temperature.[3]

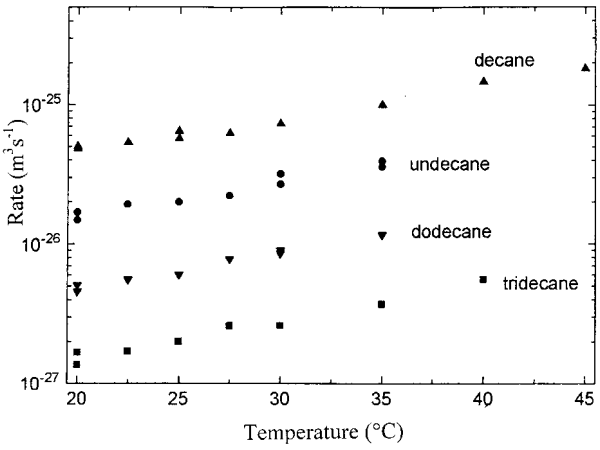

Figure 1. Ostwald ripening rates as a function of temperature for systems based on decane, undecane, dodecane and tridecane.

The rate of ripening in diluted microemulsions has been investigated by following the average droplet size with time using dynamic light scattering. The microemulsion used was one for which the dilution process has been studied in some detail in earlier papers and consisted of SDS + pentanol + water + n-alkane (10.5 + 15 + 59.5 + 15 by mass) which was diluted 50-fold into water.[4,5] Rates have been measured as functions of both temperature and of micellar and electrolyte concentration.

Rates are plotted as a function of temperature for systems containing decane, undecane, dodecane and tridecane in Fig 1. The rate increases with temperature, and this may be explained by considering the effect of temperature on each of the variables listed above. The various thermodynamic quantities of dissolution of the alkanes into water, $\Delta G°$, $\Delta H°$ and $\Delta S°$, can be determined by calculating their aqueous solubility at each temperature using the LSW equation describing Ostwald ripening.[3] The solubility (expressed as a mole fraction x_2) gives the free energy of dissolution directly ($\Delta G° = RT \ln x_2$) whilst the variation of the solubility with temperature gives the enthalpy

$$\Delta H° = -R\left(\frac{\partial \ln x_2}{\partial(1/T)}\right) \quad (4)$$

The entropy is then simply obtained from $\Delta G° = \Delta H° - T\Delta S°$. The values obtained at 25 °C, listed in table 1, agree with those in the literature for lower

Table 1. Aqueous solubility (c_∞), free energy, enthalpy and entropy of dissolution of n-alkanes in water at 25 °C obtained from Ostwald ripening rates

No. of CH_2 groups in alkanes	Aqueous solubility c_∞ ($kg\,m^{-3} \times 10^{-6}$)	$\Delta G°$ ($kJ\,mol^{-1}$)	$\Delta H°$ ($kJ\,mol^{-1}$)	$\Delta S°$ ($JK^{-1}mol^{-1}$)
10	54	46.5	7.5	−130
11	17	49.9	14.3	−119
12	3.5	53.6	18.4	−118
13	1.2	56.6	21.0	−119

members of the n-alkane family.[6] The solubility of n-alkanes falls by a factor of around 3 for each additional CH_2 group; this fall is reflected in the rates shown in Fig 1. Plots of $\Delta G°$ and $\Delta H°$ as a function of the number (n) of carbons in the alkane chain are linear, confirming that a group contribution law applies, in that each additional CH_2 group adds a constant amount of energy to the process.

The rate of ripening is dependent on the solubility of the oil in the aqueous phase, and so micelles (through solubilisation) might be expected to increase the rate. The rate of ripening was measured as a function of SDS concentration (0–2%) at several sodium chloride concentrations (0–0.2 mol dm^{-3}). The presence of sodium chloride reduced the interfacial tension in the emulsion, and, to remove this effect, rates were normalised to that at the CMC of the SDS/ pentanol mixture (0.18% in the absence of added electrolyte). This allowed the effects of micelles to be studied in isolation.

The presence of micelles has relatively little effect on the rate of ripening, with the rate typically increasing by a factor of around 2 at 2% SDS; the rate is still mainly governed by the alkane aqueous solubility. For the micelles to affect the rate significantly they must rapidly absorb the material dissolving from small droplets into the micellar core and transport them to large droplets for redeposition. The small dependence of rate on micellar concentration suggests that the oil is not rapidly taken up into the micelles – this may be due to electrostatic repulsion between the micelles and SDS molecules adsorbed on the droplets preventing close approach. Addition of sodium chloride initially increases the effect of the micelles through depression of the electrostatic repulsion between the droplets and the micelles. At higher concentrations this effect decreases as the increased solubilisation capacity of the micelles competes with the Ostwald ripening.

In summary – temperature-insensitive microemulsions may be prepared using ionic/ non-ionic surfactant mixtures. Simple modelling of the natural curvature leads to a predictive model for the optimum composition. Dilution of O/W microemulsions containing a single oil leads to droplet growth by Ostwald ripening. While the rate is sensitive to temperature, micellar or electrolyte concentration, the dominant factor is the aqueous solubility of the oil.

REFERENCES

1 Binks BP, Fletcher PDI and Taylor DJF, *Langmuir* **13**:7030 (1997).
2 Taylor P, *Colloids Surfaces* **99**:175–185 (1995).
3 Taylor P, *Adv Colloid Interface Sci* **75**:107–163 (1998).
4 Taylor P and Ottewill RH, *Colloids Surfaces* **88**:303–316 (1994).
5 Taylor P and Ottewill RH, *Prog Colloid Polymer Sci* **97**:199–203 (1994).
6 Abraham MH, *J Chem Soc Faraday Trans I*, **80**:153 (1984).

Drift reduction and droplet-size in sprays containing adjuvant oil emulsions

Nigel M Western,[1]* Eric C Hislop,[1] Marc Bieswal,[1] Peter J Holloway[1] and David Coupland[2]
[1]*IACR-Long Ashton Research Station, Department of Agricultural Sciences, University of Bristol, Long Ashton, Bristol BS41 9AF, UK*
[2]*Croda Chemicals Ltd, Cowick Hall, Snaith, Goole, North Humberside DN14 9AA, UK*

Abstract: The droplet-sizes and drift produced by sprays containing dilute oil-in-water emulsions of various vegetable and mineral oil adjuvants were measured in wind-tunnel experiments. When compared with water or a surfactant solution, both types of oil adjuvant reduced the proportion of small driftable droplets and, hence, reduced measured spray drift. Vegetable oils were more effective at drift reduction than the mineral oil. Spray drift tended to increase with increasing oil concentration and decreasing emulsifier content.

Keywords: adjuvant oils; oil-in-water emulsions; spray drift; droplet-size; spray quality

Emulsions of adjuvant oils are often added to pesticide formulations to enhance their biological activity, especially when the pesticides are used at reduced dose rates. However, their influence on the safety and efficiency of the spray application process is poorly understood. In addition, there are growing concerns about the biodegradability of mineral oil adjuvants and substitutes based on renewable and more environmentally acceptable vegetable oils are becoming of increasing importance.

In the present work, we have measured the drift potential of emulsion formulations of three oils supplied by Croda Chemicals Ltd, UK: alkali-refined rapeseed oil (ARRO), methylated rapeseed oil (MRO) and a mineral oil (MO). These were selected from a short list of seven oils (one mineral, three rapeseed and three linseed), based on their performance in biological efficacy experiments.[1] All oils were formulated as ECs containing 50 g litre^{-1} of a 5 EO oleyl alcohol as emulsifier. Oil concentrations in the spray liquid were 2, 10 and 20 g litre^{-1}, and 0.2 g litre^{-1} sodium fluorescein was added as a tracer for quantification of drift. Comparisons were made with water, the emulsifier alone and a 1 g litre^{-1} aqueous solution of a 10 EO nonylphenol surfactant ('Agral', ex Zeneca, UK).

Airborne spray drift was measured 2 m down-wind of a single, stationary 11002 nozzle (Lurmark, UK) atomiser with an output of 0.64 litre min^{-1} in a wind speed of 2.5 m s^{-1}. The nozzle was positioned so that its long axis was at 90° to the wind direction. Drift was collected according to an established protocol[2] on five

* Correspondence to: NM Western, IACR-Long Ashton Research Station, Department of Agricultural Sciences, University of Bristol, Long Ashton, Bristol BS41 9AF, UK
(*Received 8 July 1998; accepted 1 February 1999*)